Single-Molecule Characterization of the Dynamics of Calmodulin Bound to Oxidatively Modified Plasma-Membrane Ca^{2+}-ATPase†

Kenneth D. Osborn,‡ Asma Zaidi,§ Ramona J. Bieber Urbauer,||,⊥ Mary L. Michaelis,§ and Carey K. Johnson*,‡

Department of Chemistry, University of Kansas, 1251 Wescoe Hall Drive, Lawrence, Kansas 66045, Department of Pharmacology and Toxicology, University of Kansas, 1251 Wescoe Hall Drive, Lawrence, Kansas 66045, and Department of Molecular Biosciences, University of Kansas, 1200 Sunnyside, Lawrence, Kansas 66045

Received March 16, 2005; Revised Manuscript Received June 10, 2005

ABSTRACT: We used single-molecule fluorescence spectroscopy to probe the conformation of calmodulin (CaM) bound to oxidatively modified plasma-membrane Ca^{2+}-ATPase (PMCAox). We found that oxidative modification altered the coupling between the ATP binding domain and the autoinhibitory domain. Oxidative modification of PMCA is known to result in a loss of activity for the enzyme. Conformations of PMCAox−CaM complexes were probed by single-molecule polarization modulation spectroscopy, which measured the orientational mobility of fluorescently labeled CaM bound to PMCAox. We detected an enhanced population of PMCAox−CaM complexes with a low orientational mobility in the presence of ATP, whereas nonoxidized PMCA−CaM complexes existed almost exclusively in a high-mobility state in the presence of ATP. We have previously attributed such high-mobility states to PMCA−CaM complexes with a dissociated autoinhibitory/CaM binding domain, whereas the lower-mobility state was attributed to autoinhibited PMCA−CaM complexes with a nondissociated autoinhibitory domain [Osborn, K. D., et al. (2004) *Biophys. J. 87*, 1892−1899]. In the absence of ATP, the orientational mobility distributions are similar for CaM complexed with oxidized PMCA or nonoxidized PMCA. These results suggest that oxidative modification of PMCA reduced the propensity of the autoinhibitory domain to dissociate from binding sites near the catalytic core of the enzyme with bound nucleotide upon CaM stimulation in the presence of Ca^{2+}. This interpretation was further supported by chymotrypsin proteolysis, which probes the tightness of binding of the autoinhibitory domain to sites near the catalytic core of the enzyme. Enhanced proteolysis was observed for PMCA upon binding CaM or ATP. In contrast, proteolysis was partially blocked for oxidatively modified PMCA, even in the presence of ATP.

The plasma-membrane Ca^{2+}-ATPase (PMCA)[1] is a transmembrane calcium pump that functions to maintain calcium homeostasis in all eukaryotic cells (*1*, *2*). Because of its high affinity for Ca^{2+}, it is believed to play an important role in the maintenance of the >10000-fold Ca^{2+} gradient across the plasma membrane of cells. PMCA is ∼138 kDa in size with 10 transmembrane helices and several functional domains in the cytosolic portion of the protein (*3*). A large intracellular loop located between transmembrane segments 4 and 5 contains the ATP binding site and a phosphorylatable aspartate residue. The activity of PMCA is regulated by an autoinhibitory domain located near the C-terminus of the enzyme (*4*). In the inactive enzyme, this domain is believed to associate with the catalytic core containing the nucleotide and phosphorylation domains of the enzyme, thus blocking its ability to bind or utilize ATP (*5*−*8*). PMCA has been proposed to pump Ca^{2+} via a mechanism characteristic of P-type ATPases that couples ATP binding and subsequent autophosphorylation of a conserved aspartate residue on the enzyme with conformational changes that alter the Ca^{2+} binding affinity and the intracellular and extracellular access to Ca^{2+} binding sites (*9*, *10*). On the basis of recent X-ray crystallographic structures, long-range domain motions of the nucleotide binding domain and the actuator domain have been postulated for the highly homologous Ca^{2+} pump, the sarco(endo)plasmic reticulum Ca^{2+}-ATPase (SERCA) (*11*, *12*). Similar conformational motions may occur in PMCA.

PMCA activity is stimulated severalfold by the ubiquitous cellular Ca^{2+} sensor protein calmodulin (CaM), a water soluble, 16.7 kDa, Ca^{2+}-binding protein that is involved in a wide variety of signaling pathways in eukaryotic cells. After four Ca^{2+} ions bind via a pair of EF-hand binding motifs present in each of its two lobes, a hydrophobic cleft is

† This work was supported by NIH Grants R01 GM58715, AG 12993, and RR-P20 RR17708 and the American Heart Association (0455487Z).

* To whom correspondence should be addressed. E-mail: ckjohnson@ku.edu. Phone: (785) 864-4219. Fax: (785) 864-5396.

‡ Department of Chemistry.

§ Department of Pharmacology and Toxicology.

|| Department of Molecular Biosciences.

⊥ Current address: Department of Biochemistry and Molecular Biology, University of Georgia, Athens, GA 30602.

[1] Abbreviations: APD, avalanche photodiode; CaM, calmodulin; CaM-TMR, calmodulin fluorescently labeled with tetramethylrhodamine; EDTA, ethylenediaminetetraacetic acid; DTT, dithiothreitol; EGTA, ethylene glycol bis(2-aminoethyl ether)-*N*,*N*,*N*′,*N*′-tetraacetic acid; HEPES, *N*-(2-hydroxyethyl)piperazine-*N*′-(4-butanesulfonic acid); NBT/BCIP, nitro blue tetrazolium/5-bromo-4-chloro-3-indolyl phosphate; PMCA, plasma-membrane Ca^{2+}-ATPase; P_i, inorganic phosphate; PVDF, polyvinylidene fluoride; SDS−PAGE, sodium dodecyl sulfate−polyacrylamide gel electrophoresis; TMR, tetramethylrhodamine 5-maleimide.

10.1021/bi050488m CCC: $30.25
Published on Web 07/30/2005

exposed in each lobe, allowing CaM to recognize and bind a diverse range of targets, including PMCA. CaM binding to the autoinhibitory domain of PMCA leads to its dissociation from the active site, removing self-inhibition of the enzyme (*4*).

One of the most common perturbations found in cells subjected to oxidative stress is a significant alteration in cellular Ca^{2+} homeostasis (*13*−*15*). It has been shown that PMCA in synaptic plasma membranes of nerve cells is very sensitive to inactivation by a variety of reactive oxygen species (*16*). More recently, it was demonstrated that a brief exposure of the purified PMCA to moderate levels of hydrogen peroxide (H_2O_2) resulted in functional inactivation and structural changes in the protein (*17*). The weakened ability of stressed cells to achieve the low Ca^{2+} levels characteristic of healthy cells has been implicated in the process of aging and in a number of neurodegenerative disorders such as Alzheimer's disease and Parkinson's disease and in ischemia reperfusion injury (*18*). These findings raise the question of the structural and mechanistic basis for the loss of PMCA activity.

In this study, we used single-molecule polarization modulation experiments to investigate the dynamics of the interaction between the catalytic core and the CaM-binding domain of oxidatively modified PMCA (PMCAox). Single-molecule methods provide a means of exploring the function and dynamics of individual molecules in heterogeneous systems. In polarization modulation experiments, the polarization of the excitation beam is continuously rotated, and the extent of modulation in the subsequent fluorescence is monitored (*19*−*25*). For an orientationally immobile fluorophore, the absorption probability of the molecule is modulated by the rotating excitation polarization. In contrast, a rapidly reorienting molecule experiences little or no modulation of excitation. Thus, highly modulated emission of the probe indicates a low mobility of the labeled portion of the protein, whereas unmodulated emission indicates a high orientational mobility.

In our laboratory, we used single-molecule polarization modulation experiments to explore the single-molecule dynamics of the Ca^{2+}-dependent activation of PMCA by CaM, which was labeled with the fluorescent dye tetramethylrhodamine (TMR) (*26*, *27*). At a Ca^{2+} concentration of 25 μM, sufficient for full activation of PMCA by CaM, we observed a high orientational mobility of CaM-TMR bound to PMCA, consistent with a dissociated autoinhibitory domain (*28*). In contrast, at a lower Ca^{2+} concentration (0.15 μM), a population of PMCA−CaM complexes with low mobility appeared. We attributed this population to inactive PMCA−CaM complexes with a nondissociated autoinhibitory domain (*26*). These results suggested that the orientational mobility of CaM-TMR bound to PMCA, as determined in single-molecule polarization modulation experiments, tracks the conformation of the autoinhibitory domain of PMCA, signaling whether it is associated or dissociated from the catalytic site of the enzyme. Proteolytic cleavage profiles for PMCA presented in the present paper support this interpretation. We further found that oxidative modification of CaM results in an enhanced population having a low orientational mobility, suggesting that although oxidatively modified CaM can bind to the autoinhibitory domain of PMCA, it does not effectively induce dissociation of the autoinhibitory domain, resulting in a loss of CaM-stimulated PMCA activity (*27*).

In the paper presented here, we report an enhanced population of PMCAox−CaM-TMR complexes with decreased orientational mobility in the presence of ATP compared to that of native PMCA−CaM-TMR complexes, suggesting an increased population of complexes with a nondissociated autoinhibitory domain in PMCAox−CaM complexes. These results were further supported by limited proteolysis experiments that showed a decreased accessibility of the protease chymotrypsin to its cut site in the autoinhibitory domain for PMCAox in the presence of ATP compared to native PMCA. These results suggest that the loss of activity in oxidatively modified PMCA resulted at least in part from altered interactions between the catalytic core and the autoinhibitory domain and a reduced potency of CaM in inducing dissociation of the autoinhibitory domain.

MATERIALS AND METHODS

Materials. Chicken CaM was mutated to replace a threonine residue at position 34 with a cysteine as previously described (*29*). T34C-CaM was labeled with tetramethylrhodamine 5-maleimide (TMR) (Molecular Probes, Eugene, OR) according to standard protocols from the manufacturer. This labeling occurred at >90% efficiency as determined by mass spectrometry and integration of peaks after HPLC purification. After dye labeling, CaM-TMR (1 mg) was dialyzed three times against 4 L of a buffer consisting of 10 mM 4-(2-hydroxyethyl)-1-piperazineethanesulfonic acid (HEPES), 0.1 M KCl, 1 mM $MgCl_2$, and 0.1 mM $CaCl_2$ to remove any unreacted dye. After dialysis, the concentration of the resultant stock solution of CaM-TMR was 78 μM.

PMCA was purified from freshly drawn human blood by affinity chromatography on a CaM−Sepharose column and stored at −80 °C. The enzyme was eluted off the column in a buffer containing 10 mM HEPES (pH 7.2), 120 mM NaCl, 1 mM $MgCl_2$, 2 mM ethylenediaminetetraacetic acid (EDTA), 0.5 mg/mL phosphatidylcholine, 0.05% $C_{12}E_8$, and 5% (v/v) glycerol. Active fractions were pooled, and appropriate amounts of $MgCl_2$ and $CaCl_2$ were added to neutralize the EDTA (*30*). Buffer conditions used for single-molecule experiments were based on a standard 10 mM HEPES buffer (pH 7.4) with 0.1 M KCl, 1 mM $MgCl_2$, and 0.214 mM $CaCl_2$. This yielded 1 mM free Mg^{2+} and 25 μM free Ca^{2+} in the final sample solution as calculated with a computer program (*11*) that takes into account the EDTA, Ca^{2+}, and Mg^{2+} added by the PMCA storage buffer. Calcium buffers with 0.15 μM free Ca^{2+} were the same as that described above with the addition of 10 mM ethylene glycol bis(2-aminoethyl ether)-*N*,*N*,*N*′,*N*′-tetraacetic acid (EGTA) and appropriate adjustments in the added $MgCl_2$ and $CaCl_2$ to yield the desired free ion concentrations. Chymotrypsin was purchased from Sigma Chemical Co. and the pan PMCA antibody from Affinity Bioreagents. All other reagents were of the highest commercially available quality.

Samples for the single-molecule studies were made by premixing 2 μL of a 0.1 μM purified PMCA sample with 5 μL of 2 nM CaM-TMR. The mixture was allowed to bind at room temperature for at least 15 min. In measurements with nucleotide, ATP (1 mM) was added immediately prior to mixing of this sample with a melted 3% agarose solution

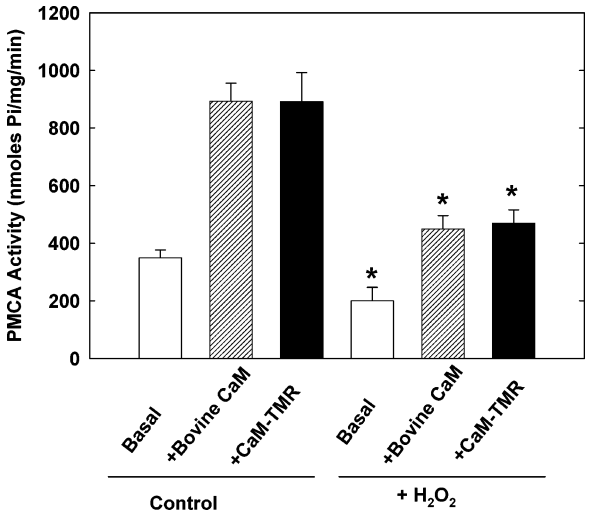

FIGURE 1: Stimulation of PMCA activity by CaM-TMR. The activity of control and oxidized PMCA was determined as described in Materials and Methods in the absence and presence of 120 nM CaM-TMR or bovine brain CaM. Data represent the mean values from three experiments with triplicate samples. Error bars represent the standard error of the mean. The statistical significance of differences between control and H_2O_2-treated samples was determined with a Student's *t* test (asterisk denotes $p < 0.01$).

as the experiments required. The PMCA−CaM sample was mixed rapidly with the agarose at ~43 °C, just above the gelling temperature, and then transferred quickly to a clean glass coverslip prechilled to 4 °C to trap PMCA in the gel and to minimize its exposure to elevated temperatures. This mixture was allowed to sit on ice until the gel had completely formed before the sample was covered with a second clean glass coverslip and transferred to the microscope for data collection.

Oxidative Modification of PMCA. Aliquots of the purified PMCA were exposed to 100 μM H_2O_2 for 10 min at 37 °C as described previously (*17*). The reaction was terminated by the addition of 2 units of catalase, and tubes were incubated for 5 min at 23 °C to allow the remaining H_2O_2 to decompose.

PMCA Activity Assays. The activity of PMCA was determined in 96-well microplates as described previously (*17*). Briefly, each well contained the following in a final volume of 100 μL: 25 mM Tris-HCl (pH 7.4), 50 mM KCl, 1 mM $MgCl_2$, 0.1 mM ouabain, 4 μg/mL oligomycin, 200 μM EGTA, and enough $CaCl_2$ added to yield a final free Ca^{2+} concentration of 10 μM. The PMCA activity measured in the presence of Ca^{2+} but without CaM is termed the "basal" activity and that in the presence of Ca^{2+} and 120 nM CaM (bovine brain or recombinant TMR-labeled) the "CaM-stimulated" activity. After a 5 min preincubation of the PMCA with other components of the assay, the reaction was started by the addition of 1 mM ATP (or as indicated in the figure legends; see Figure 1), continued for 20 min at 37 °C, and stopped by the addition of Malachite Green dye (*31*). The contents were made acidic by addition of 19.5% H_2SO_4 and incubated for 45 min, and the color was read at 650 nm in a microwell plate reader. The PMCA activity was defined as the Ca^{2+}-activated ATP hydrolysis and expressed as nanomoles of inorganic phosphate liberated per milligram of protein per minute, based on values from a standard curve of the absorbance using various concentrations of free inorganic phosphate.

Single-Molecule Instrumentation. CaM-TMR was excited with a linearly polarized, 543 nm helium−neon laser. The beam from this laser was passed through a laser intensity stabilizer (CR-200-A, Thorlabs), followed by a high-precision linear polarizer. The polarization was modulated by an electro-optic modulator (M-350, ConOptics) driven by ramp waveforms generated by a function generator (DS 340, Stanford Research Systems) at 25 Hz. In combination with an achromatic quarter waveplate (Karl-Lambrecht), the electro-optic modulator produces a linearly polarized beam in which the orientation of the polarization rotates continuously at the frequency set by the function generator. The beam was expanded and collimated to backfill the microscope objective for optimal resolution. A variable neutral density filter and narrow excitation band-pass filter (D543/10x, Chroma) were used to reduce the beam intensity to ≤1 μW. The beam was directed into the epi-illumination port of a Nikon TE300 inverted microscope where it was reflected by a dichroic mirror (Q555LP, Chroma) into a 1.3 NA, oil-immersion objective (Nikon, SuperFluor). The sample was held on a microscope coverslip located on a piezo-electric scanning stage (Nano-H100, Mad City Labs). Fluorescence collected by the objective lens was transmitted through the dichroic mirror and an emission filter (HQ600/80m, Chroma) before detection by an avalanche photodiode (APD) (Perkin-Elmer Optoelectronics SPCM-AQR-14).

Data Collection and Analysis. The gel was scanned for single molecules by the piezo-electric nanopositioning stage. A PCI-6052E card (National Instruments) was used to control the nanopositioning stage and to register counts from the APD. After single molecules were located, the stage was positioned with the single molecule in the focus of the excitation beam, and fluorescence trajectories were collected with a PCI-6602 card (National Instruments). A maximum-likelihood analysis method described previously (*25*) was used to fit modulated trajectories period by period. The modulation depth (defined as the fraction of the overall intensity that is modulated) for each molecule was averaged over the entire trajectory to characterize the orientational mobility of single PMCA−CaM-TMR complexes.

Digestion of PMCA by Chymotrypsin and Immunoblotting. Five micrograms of purified PMCA was preincubated for 3 min at 37 °C in a buffer containing 10 mM HEPES (pH 7.2), 120 mM NaCl, 1 mM $MgCl_2$, 0.5 mg/mL phosphatidylcholine, 0.05% $C_{12}E_8$, 5% (v/v) glycerol, 5 mM DTT, 0.1 mM EGTA, 25 μM free Ca^{2+} (when added), 500 nM CaM (when added), and 1 mM ATP (when added). The proteolysis was initiated by the addition of 0.05 μg/mL α-chymotrypsin and stopped after 10 min at 37 °C by the addition of ice-cold trichloroacetic acid (6% final concentration) (*7*, *8*). The pellet was supplemented with 100 μg of bovine serum albumin, washed once with water, and dissolved in SDS−PAGE sample buffer [62.5 mM Tris-HCl (pH 6.8), 2% SDS, 10% glycerol, 5 mM EDTA, 100 mM DTT, and 125 mg/mL urea]. The samples were subsequently run on 7.5% polyacrylamide gels, electroblotted to PVDF membranes, and immunostained with a pan PMCA antibody (1:1000). Alkaline phosphatase-conjugated secondary antibody and NBT/BCIP were used to visualize the PMCA bands that were scanned in Adobe Photoshop 8.0.

RESULTS

CaM-Dependent Activation of Oxidatively Modified PMCA. PMCA activity assays were performed to characterize the activation of PMCAox by CaM-TMR relative to that of native PMCA. Bovine brain CaM was used as a reference in these experiments. The results are shown in Figure 1. As observed previously, a 10 min exposure of PMCA to 100 μM H_2O_2 resulted in an ~50% decline in both basal and CaM-stimulated PMCA activity (*17*). The effectiveness of CaM-TMR in stimulating both native and oxidized PMCA was comparable to that of bovine brain CaM. This demonstrates that the substitution of threonine for cysteine in the recombinant CaM and the labeling of cysteine with TMR did not affect the biological characteristics of CaM as measured by its stimulation of PMCA activity (Figure 1).

Calcium Dependence of Oxidized PMCA. CaM-TMR was added to samples of PMCAox immobilized in an agarose gel with a Ca^{2+} concentration of 0.15 μM (low Ca^{2+}) or 25 μM (high Ca^{2+}) as described in Materials and Methods. Single PMCAox−CaM-TMR complexes were located by scanning a 10 μm × 10 μm area of the gel in a region several micrometers above the surface of the coverslip. We have previously found that CaM-TMR is not immobilized in an agarose gel in the absence of PMCA and Ca^{2+} (*25*). Thus, single CaM-TMR molecules detected with restricted translational mobility are bound to PMCA in a Ca^{2+}-dependent manner. Fluorescence trajectories were recorded for single PMCAox−CaM-TMR complexes as described previously (*25*). Via a determination of the depth of modulation of fluorescence, the orientational mobility was characterized in single-molecule fluorescence trajectories as described previously (*25*). Anisotropy decay measurements showed that TMR was reorientationally coupled to CaM in CaM-TMR with only a small degree of motion independent of CaM, indicating that TMR reorientation is largely restricted relative to CaM (*26*). Thus, TMR reports the orientational mobility of CaM. We have applied these techniques previously to complexes of native PMCA with CaM-TMR and oxidized CaM-TMR (*26*, *27*).

Polarization modulation trajectories were recorded at Ca^{2+} concentrations of 0.15 and 25 μM. In most cases, the orientational mobility of a given PMCA−CaM-TMR complex is static on the time scale of a fluorescence trajectory (*26*). Therefore, each molecule observed was characterized by its average modulation depth. Histograms of average modulation depths determined in this way are shown in panels A and B of Figure 2. For comparison, the modulation depth distributions determined previously (*26*) for native PMCA−CaM-TMR complexes at Ca^{2+} concentrations of 0.15 and 25 μM are also shown in panels C and D of Figure 2. Zaidi and co-workers found a slight increase in the extent of binding of CaM to PMCAox compared to that for native PMCA (*17*). Thus, the increased low-mobility population for the PMCAox−CaM-TMR complex does not result from reduced tightness of binding of CaM to PMCAox.

The modulation depth distributions for CaM-TMR complexes with PMCAox at both 0.15 and 25 μM show the presence of a population with a high orientational mobility. This population peaks at a modulation depth of 0.40. A number of complexes, however, display a higher modulation depth, indicating a lower orientational mobility with a modulation depth of >0.50. The presence of a population of PMCAox−CaM-TMR complexes having a lower orientational mobility was more pronounced at a Ca^{2+} concentration of 0.15 μM than at 25 μM (Figure 2A,B). This result is consistent with measurements previously reported for native PMCA−CaM-TMR complexes (*26*) (Figure 2C,D). For each molecule, the uncertainty in the modulation depth was estimated to be ±0.03 to ±0.05. Therefore, the width of the high-mobility population is predominantly a result of experimental uncertainty. However, the low-mobility population exhibits a broader distribution of mobilities, suggesting heterogeneity at the molecular level.

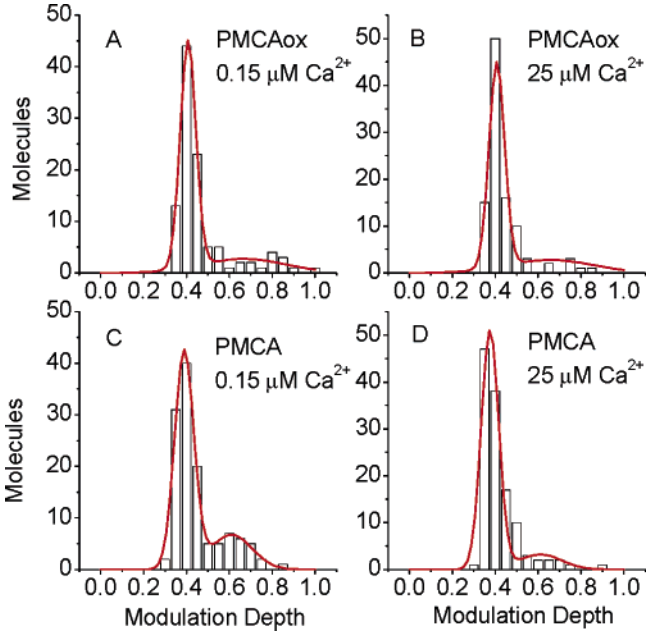

FIGURE 2: Histograms of modulation depths of CaM-TMR bound to oxidized PMCA at (A) 0.15 and (B) 25 μM Ca^{2+} or to native PMCA at (C) 0.15 and (D) 25 μM Ca^{2+} in the absence of ATP. The solid lines show fits of the high-mobility population to double-Gaussian distributions with peak positions at modulation depths of (A) 0.41 and 0.67, (B) 0.41 and 0.66, (C) 0.41 and 0.61, and (D) 0.38 and 0.61.

As a means of comparing the distributions of the two populations, it is instructive to compare the fraction of molecules with high and low modulation depths. A convenient threshold level for comparison purposes is 0.5. For native PMCA, the fraction of the population with a modulation depth above 0.5 is 9% at 25 μM Ca^{2+}. This fraction increases to 21% at 0.15 μM Ca^{2+}, showing the increased population with a low mobility at the reduced Ca^{2+} concentration. For PMCAox, the fraction of the population with a modulation depth above 0.5 was 10% at 25 μM Ca^{2+} and 19% at 0.15 μM Ca^{2+}. Thus, these fractions were not significantly different from the populations for native PMCA, suggesting that the dynamics of the CaM binding domain of PMCA detected via polarization modulation depths are not strongly affected by oxidation.

ATP Dependence of Oxidized PMCA. ATP is required as a source of metabolic energy for PMCA−CaM complexes to function in a cellular environment. Binding of ATP to the nucleotide binding site of PMCA drives enzymatic turnover, resulting in phosphorylation of a conserved aspartate residue followed by protein conformational changes, subsequent release of inorganic phosphate (P_i), and the

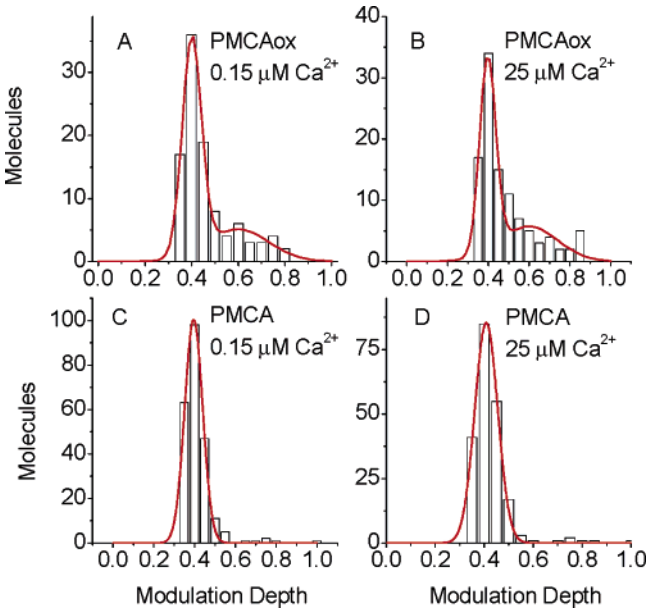

FIGURE 3: Histograms of modulation depths of CaM-TMR bound to oxidized PMCA at (A) 0.15 and (B) 25 μM Ca^{2+} or to native PMCA at (C) 0.15 and (D) 25 μM Ca^{2+} in the presence of 1 mM ATP. The solid lines show fits of the high-mobility population to double-Gaussian distributions with peak positions at modulation depths of (A and B) 0.40 and 0.60, (C) 0.40, and (D) 0.41.

transport of Ca^{2+} from the cytoplasmic to the exoplasmic side of the plasma membrane. Panels A and B of Figure 3 show polarization modulation histograms for the PMCAox−CaM-TMR complex in the presence of 1 mM ATP. The corresponding histograms for native PMCA are shown for comparison [Figure 3C,D (*26*)]. For nonoxidized PMCA−CaM-TMR complexes, we previously noted that the presence of ATP results almost exclusively in a high-mobility population with an average modulation depth of ~0.40 and a very low (6%) population having a modulation depth of >0.5, even at a reduced Ca^{2+} concentration, suggesting that ATP binding or utilization favors dissociation of the autoinhibitory domain (*26*). In contrast, for PMCAox−CaM-TMR complexes in the presence of ATP, 22% of the molecules had a modulation depth greater than 0.5 at a Ca^{2+} concentration of 0.15 μM and 27% of the molecules had a modulation depth greater than 0.5 at a Ca^{2+} concentration of 25 μM. The population of the immobile state for PMCAox at both Ca^{2+} concentrations in the presence of ATP (Figure 3A,B) was comparable to that of the low-mobility state observed in native PMCA and PMCAox at 0.15 μM Ca^{2+} in the absence of ATP (Figure 2A,C). Thus, for PMCAox, the presence of the nucleotide did not eliminate the immobile state of the PMCAox−CaM complex, in contrast to the effect of the nucleotide for the nonoxidized PMCA−CaM-TMR complex. In fact, the low-mobility fraction for PMCAox increased at high Ca^{2+} concentrations in the presence of ATP (Figure 3B) relative to that for PMCAox in the absence of ATP (Figure 2B), whereas the presence of ATP for native PMCA at high Ca^{2+} concentrations resulted in a decrease in the low-mobility fraction (Figure 3D vs Figure 2D). These data suggest that the interaction between the catalytic core of PMCAox and its autoinhibitory domain in the presence of ATP at high Ca^{2+} concentrations is altered as a result of oxidation of PMCA.

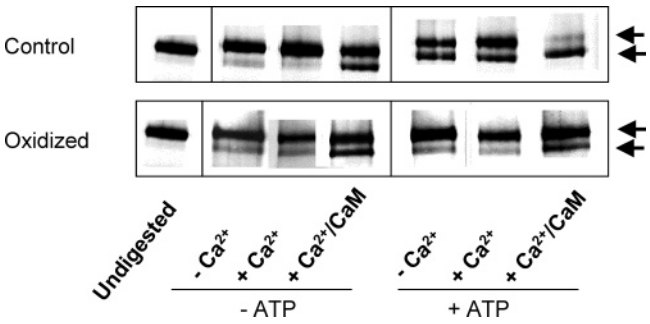

FIGURE 4: Immunoblots showing the susceptibility of PMCA to proteolysis. Five micrograms of PMCA (control and oxidized) was digested with chymotrypsin for 10 min at 37 °C as described in Materials and Methods. Digestion was performed in the absence of Ca^{2+}, in the presence of 25 μM Ca^{2+}, or in the presence of 25 μM Ca^{2+} and 500 nM CaM. The final concentration of ATP when added was 1 mM. Proteolysis was terminated by TCA (6% final concentration), and the pellet was resuspended in SDS−PAGE sample buffer, loaded on a 7.5% polyacrylamide gel, and immunoblotted with anti-PMCA antibody (1:1000).

The immobile population in the presence of ATP at high Ca^{2+} concentrations increases from 6% in native PMCA (Figure 3D) to 27% in PMCAox (Figure 3B). This result can be compared to the decrease in activity upon oxidative modification shown in Figure 1. The results in Figure 1 suggest that the activity loss upon oxidation has two components: one due to a roughly 50% loss in basal activity that occurs even in the absence of CaM and the other due to nonproductive CaM binding. We expect that the low-mobility fraction of PMCAox−CaM-TMR complexes measured by single-molecule polarization modulation reflects PMCAox molecules that were inactive due to nonproductive CaM binding. The total activity in the presence of CaM-TMR decreased from 907 ± 42 nmol of P_i mg^{-1} min^{-1} for PMCA to 473 ± 14 nmol of P_i mg^{-1} min^{-1} for PMCAox. The basal activity in the absence of CaM decreased from 351 ± 18 nmol of P_i mg^{-1} min^{-1} for PMCA to 200 ± 20 nmol of P_i mg^{-1} min^{-1} for PMCAox, corresponding to a loss of 151 ± 27 nmol of P_i mg^{-1} min^{-1}, indicating oxidation-induced impairment in the PMCA catalytic cycle that is independent of CaM activation. This may represent a fraction of the high-mobility PMCAox population that is functionally inactive, or it may reflect a decrease in the rate of enzyme function in the high-mobility fraction. The remaining activity loss was attributable to nonproductive CaM binding. This corresponds to a loss of 283 ± 52 mol of P_i mg^{-1} min^{-1} out of a total of 907 nmol of P_i mg^{-1} min^{-1}, or 31%. This fraction is in good agreement with the low-mobility fraction of the PMCAox−CaM-TMR population in the presence of ATP and high Ca^{2+} concentrations, and thus in agreement with the expectation that it represents activity loss resulting from nonproductive CaM binding.

Proteolysis of PMCAox. The access of α-chymotrypsin to its cleavage site on the autoinhibitory domain of PMCA has been recently used as a sensitive measure of regulatory interactions within different conformational states of the protein (*7*, *8*). Chymotrypsin cleaves the ~138 kDa intact PMCA downstream of the CaM binding domain, giving rise to a major fragment of ~125 kDa (*7*). The lack of proteolytic cleavage of intact PMCA by chymotrypsin was thought to indicate a tight interaction of the autoinhibitory region with the nucleotide binding catalytic core (*7*). Figure 4 shows the

degradation pattern of control and oxidized PMCA following a 10 min exposure to chymotrypsin as described in Materials and Methods. In accordance with previous observations, there was minimal proteolysis of native PMCA in the presence of EGTA or 25 μM free Ca^{2+}, consistent with the closed state of PMCA (*7*, *8*). Addition of Ca^{2+}-bound CaM significantly accelerated the proteolysis, and a distinct ~125 kDa fragment of PMCA could be seen. Interestingly, we found that when PMCA digestion was performed in the presence of 1 mM ATP, the proteolysis was accelerated in all three cases, i.e., absence of Ca^{2+}, presence of Ca^{2+}, and presence of Ca^{2+}-bound CaM, suggesting that binding of nucleotide to the PMCA or its utilization favors the dissociation of the autoinhibitory domain and hence an open conformation. The proteolytic profile of the oxidized PMCA in the absence of ATP was comparable to the control; however, in the presence of ATP, there was no further increase in the level of PMCAox breakdown, in contrast to the control. Thus, the pattern of proteolysis for PMCAox in the presence of ATP resembles that of native PMCA and PMCAox in the absence of ATP. The proteolysis data support our single-molecule results suggesting altered interactions between the catalytic core of PMCAox and its autoinhibitory domain in the presence of ATP.

DISCUSSION

Orientational Mobility of PMCA−CaM Complexes. Single-molecule polarization modulation experiments probe the orientational mobility of the fluorophore. Using fluorescently labeled CaM as a reporter molecule, we successfully applied this technique to obtain new information about the conformational states of PMCA−CaM complexes (*25*, *26*). The CaM binding domain of PMCA is co-extensive with a sequence near the C-terminal domain that is thought to function as an autoinhibitory domain (*4*). Binding of CaM to PMCA is thought to lead to dissociation of the autoinhibitory domain. A rotational correlation time of 80 ns was measured by Squier and co-workers for CaM bound to PMCA at a Ca^{2+} concentration of 100 μM, sufficient to saturate the activity of the enzyme; this suggests that the dissociated autoinhibitory domain is orientationally mobile with respect to the rest of the protein (*28*). We therefore anticipated that CaM bound to PMCA would be highly mobile, as in fact we observed for the PMCA−CaM-TMR complex at a saturating Ca^{2+} concentration of 25 μM (*26*). However, at a Ca^{2+} concentration of 0.15 μM, we observed a population with lower orientational mobility. The low-mobility population observed at a Ca^{2+} concentration of 0.15 μM thus reveals the presence of a state for which a two-state model cannot account. In a two-state model, PMCA without CaM bound would exhibit only basal activity, while all PMCA−CaM complexes would be fully active with a dissociated autoinhibitory domain (*4*, *5*). We argued that the low-mobility population corresponds to PMCA−CaM complexes to which CaM is bound, but the autoinhibitory domain is not dissociated; therefore, the PMCA is not active (*26*). For PMCA−CaM complexes in the presence of ATP, the low-mobility population was not observed, even at a reduced Ca^{2+} concentration of 0.15 μM (*26*). This result suggests that association of the autoinhibitory domain with its binding sites near the catalytic site of PMCA is disrupted in the presence of ATP, either as a consequence of binding of ATP in the nucleotide binding domain or as a result of the ATP-dependent formation of subsequent states of the enzyme. This result thus indicates the existence of structural coupling between the nucleotide binding site and the autoinhibitory binding regions, as shown previously (*5*, *7*).

This interpretation is supported by the proteolytic profiles of PMCA shown in Figure 4, which indicate a change in the availability of proteolytic sites in the C-terminal domain of PMCA in the presence of ATP. Proteolysis of PMCA by chymotrypsin at a site downstream from the CaM binding domain has been interpreted to indicate a loose or dissociated autoinhibitory domain corresponding to a non-autoinhibited enzyme (*7*, *8*). Although proteolysis was inhibited in the absence of Ca^{2+}, consistent with previous results (*7*, *8*), proteolytic cleavage was extensive in the presence of ATP, even in the absence of Ca^{2+} (see Control in Figure 4). This suggests that addition of the nucleotide favors dissociation of the autoinhibitory domain. Correspondingly, in the presence of ATP, the low-mobility population is nearly absent, even at a reduced Ca^{2+} level [Figure 3C,D (*26*)], consistent with a dissociated autoinhibitory domain under those conditions.

Orientational Mobility of PMCAox−CaM Complexes. The relationship of conformation to activity in PMCAox is of considerable interest, as the locations of oxidative modification within PMCA have not yet been resolved. It is known that oxidative modification of PMCA leads to a decrease in the maximal level of activation of the PMCA−CaM system, but the mechanistic cause of the activity loss is not well understood (*17*). The modulation depth distributions observed for CaM-TMR complexes with PMCAox in the absence of ATP were not significantly different from those observed previously for complexes with native PMCA (Figure 2). This suggests that the native and oxidized forms of PMCA exhibit only minor differences with respect to the dynamics of the autoinhibitory domain in the absence of ATP, supporting the earlier results of Zaidi et al. (*17*) which showed that the CaM binding domain is itself not directly modified by H_2O_2. Consistent with this view is the finding that the proteolytic profiles for PMCAox in the absence of ATP were similar to those for native PMCA in the absence of ATP (Figure 4).

In contrast, in the presence of ATP, we detected a significant difference in the orientational mobilities of PMCAox−CaM-TMR complexes and native PMCA−CaM-TMR complexes (Figure 3). The modulation depth distributions for complexes of CaM-TMR with PMCAox in the presence of ATP revealed a significant fraction of molecules with a low orientational mobility (Figure 3A,B). In contrast, in complexes with native PMCA, the presence of ATP resulted in an almost complete absence of the low-mobility population (Figure 3C,D). The altered mobility distribution in the presence of ATP indicates that ATP binding occurred in PMCAox. The presence of orientationally immobile PMCAox−CaM-TMR complexes in the presence of ATP implies that the structural coupling between the catalytic and autoinhibitory domains that occurs upon ATP binding or utilization in native PMCA is disrupted in PMCAox. These results were further complemented by the PMCA proteolysis data showing decreased accessibility of chymotrypsin to its cleavage site on PMCAox in the presence of ATP (Figure 4), in contrast to the native enzyme in which ATP greatly facilitated proteolysis, suggesting tighter association of the

autoinhibitory domain with the catalytic core of the enzyme in PMCAox compared to native PMCA in the presence of ATP.

A further indication of the effect of oxidation on the coupling between ATP binding and the autoinhibitory domain is evident in the increase in the low-mobility population for the PMCAox−CaM-TMR complex when ATP was added at a high Ca^{2+} concentration (Figure 3B compared to Figure 2B). These results suggest that oxidation impairs the structural coupling between the nucleotide binding site and the autoinhibitory domain of PMCAox with the result that autoinhibitory domain association is enhanced in the presence of ATP. It appears that PMCAox fails to undergo the conformational changes that occur in native PMCA that promote dissociation of the autoinhibitory domain after binding of ATP. Oxidative modifications at or near the nucleotide-binding site of the PMCA, such as formation of a disulfide bond, may alter the binding geometry of ATP or constrain the PMCA conformation, enhancing a conformation of PMCA that is conducive to self-association of the autoinhibitory domain once ATP binds or is hydrolyzed. At a reduced Ca^{2+} concentration of 0.15 μM, the addition of ATP did not remove the immobile fraction of PMCAox−CaM-TMR complexes (Figure 3A) as it did for native PMCA−CaM-TMR complexes (Figure 3C), again demonstrating the altered coupling between ATP binding and the autoinhibitory domain for PMCAox.

Penniston and co-workers have established that additional interactions outside of the 30-residue CaM-binding region of the pump are required for full self-inhibition by the autoinhibitory domain (*6*). These additional interactions in the C-terminal portion of the pump are most likely involved in self-association of the autoinhibitory domain at saturating Ca^{2+} concentrations. In native PMCA, conformational changes following binding of ATP to the nucleotide binding site or subsequent ATP utilization may disrupt these interactions as suggested by the complete disappearance of the population with low orientational mobility and by the increased accessibility of chymotrypsin to its cleavage site, which is a few residues downstream of the CaM binding domain (*7*). In contrast, in PMCAox, ATP binding or utilization was apparently less effective in disrupting these interactions.

Results of Zaidi et al. have shown that the binding of CaM to PMCA prior to treatment with H_2O_2 offers protection from oxidation of PMCA (*17*). Release of the autoinhibitory domain by CaM was suggested to induce a conformational state of PMCA that is resistant to oxidative inactivation of the pump. The conformational changes responsible for protection against oxidation may occur in a state that is accessible only when the autoinhibitory domain is dissociated. Correspondingly, the results of this study indicate that oxidation impairs protein conformational changes associated with the productive utilization of ATP, thus enhancing a structure of PMCA that is conducive to self-association of the autoinhibitory domain. Oxidative modification may also impair the structural changes that occur within PMCA upon phosphorylation of the critical aspartate residue in its active site. The earlier results of Zaidi et al. showed that the only chemical change in PMCA exposed to peroxide was the oxidation of Cys residues (*17*). There are 10 cysteines located in the cytoplasmic loop between transmembrance helices 4 and 5 containing the active site. Interestingly, Cys537 is the first amino acid on the stretch of residues (537−544) comprising the receptor that interacts with the CaM binding domain (*5*, *32*). Additionally, Cys601 is a few residues from the ATP binding site at Lys591. It is possible that oxidative modification of one or more of the cysteines in this region may contribute to conformations favoring association of the CaM binding domain and nonproductive binding of ATP, leading to enzyme inactivation. This is consistent with the view that hydrolysis of ATP is coupled to structural changes that determine the binding affinity of the autoinhibitory domain, as suggested by the single-molecule orientational mobilities of native PMCA−CaM-TMR complexes (*26*) and by the susceptibility of native PMCA to chymotrypsin proteolysis in the presence of ATP, as presented here.

CONCLUSIONS

The results presented here demonstrate the utility of single-molecule measurements in probing the dynamics of PMCAox−CaM complexes in different conformational states. The results revealed an increased low-mobility population for CaM-TMR complexes with PMCAox in the presence of ATP compared to that with native PMCA. We suggested previously (*26*) that the low-mobility population is associated with inactive PMCAox−CaM-TMR complexes having a nondissociated autoinhibitory domain. This picture suggests a mechanism for the loss of PMCA activity upon exposure to H_2O_2. The increase in the orientationally immobile population of PMCAox−CaM-TMR complexes in the presence of ATP indicates that oxidative modification alters the structural coupling between the ATP binding site and the autoinhibitory domain, reducing the propensity of the autoinhibitory domain to dissociate from binding sites in the nucleotide-binding and phosphorylation domains of the enzyme, hindering the ability of the enzyme to utilize bound ATP. These data were further supported by PMCA proteolysis by chymotrypsin and activity assays in the presence of various concentrations of ATP. This study demonstrates the power of single-molecule spectroscopy, combined with traditional biochemical methods, to provide valuable insight into the mechanisms of normal and impaired enzyme function, such as that occurring with oxidative damage or biological aging.

REFERENCES

1. Carafoli, E. (1987) Intracellular Calcium Homeostasis, *Annu. Rev. Biochem. 56*, 395−433.
2. Penniston, J. T., and Enyedi, A. (1998) Modulation of the Plasma Membrane Ca^{2+} Pump, *J. Membr. Biol. 165*, 101−109.
3. Verma, A. K., Filoteo, A. G., Stanford, D. R., Wieben, E. D., Penniston, J. T., Strehler, E. E., Fischer, R., Heim, R., Vogel, G., Mathews, S., Strehler-Page, M.-A., James, P., Vorherr, T., Krebs, J., and Carafoli, E. (1988) Complete Primary Structure of a Human Plasma Membrane Ca^{2+} Pump, *J. Biol. Chem. 263*, 14152−14159.
4. Enyedi, A., Vorherr, T., James, P., McCormick, D. J., Filoteo, A. G., Carafoli, E., and Penniston, J. T. (1989) The Calmodulin Binding Domain of the Plasma Membrane Ca^{2+} Pump Interacts both with Calmodulin and with Another Part of the Pump, *J. Biol. Chem. 264*, 12313−12321.
5. Falchetto, R., Vorherr, T., Brunner, J., and Carafoli, E. (1991) The Plasma Membrane Ca^{2+} Pump Contains a Site That Interacts with Its Calmodulin-Binding Domain, *J. Biol. Chem. 266*, 2930−2936.
6. Verma, A. K., Enyedi, A., Filoteo, A. G., and Penniston, J. T. (1994) Regulatory Region of Plasma Membrane Ca^{2+} Pump. 28

Residues Suffice to Bind Calmodulin but More are Needed for Full Auto-Inhibition of the Activity, *J. Biol. Chem. 269*, 1687−1691.
7. Padanyi, R., Paszty, K., Penheiter, A. R., Filoteo, A. G., Penniston, J. T., and Enyedi, A. (2003) Intramolecular Interactions of the Regulatory Region with the Catalytic Core in the Plasma Membrane Calcium Pump, *J. Biol. Chem. 278*, 35798−35804.
8. Bredeston, L. M., and Adamo, H. P. (2004) Loss of Autoinhibition of the Plasma Membrane Ca^{2+} Pump by Substitution of Aspartic 170 by Asparagin. Activation of Plasma Membrane Calcium ATPase 4 without Disruption of the Interaction Between the Catalytic Core and the C-terminal Regulatory Domain, *J. Biol. Chem. 279*, 41619−41625.
9. Rega, A. F., and Garrahan, P. J. (1986) *Ca^{2+} Pump of Plasma Membranes*, CRC Press, Boca Raton, FL.
10. de Meis, L., and Vianna, A. L. (1979) Energy Interconversion by the Ca^{2+}-Dependent ATPase of the Sarcoplasmic Reticulum, *Annu. Rev. Biochem. 48*, 275−292.
11. Toyoshima, C., Nakasako, M., Nomura, H., and Ogawa, H. (2000) Crystal Structure of the Calcium Pump of Sarcoplasmic Reticulum at 2.6 Å Resolution, *Nature 405*, 647−655.
12. Toyoshima, C., and Nomura, H. (2002) Structural Changes in the Calcium Pump Accompanying the Dissociation of Calcium, *Nature 418*, 605−611.
13. Berridge, M. J., Lipp, P., and Bootman, M. D. (2000) The Versatility and Universality of Calcium Signaling, *Nat. Rev. Mol. Cell Biol. 1*, 11−21.
14. Sastry, P. S., and Rao, K. S. (2000) Apoptosis and the Nervous System, *J. Neurochem. 74*, 1−20.
15. Bootman, M. D., Berridge, M. J., and Roderick, H. L. (2002) Calcium Signalling: More Messengers, More Channels, More Complexity, *Curr. Biol. 12*, R563−R565.
16. Zaidi, A., and Michaelis, M. L. (1999) Effects of Reactive Oxygen Species on Brain Synamptic Plasma Membrane Ca^{2+}-ATPase, *Free Radical Biol. Med. 27*, 810−821.
17. Zaidi, A., Barron, L., Sharov, V. S., Schoneich, C., Michaelis, E. K., and Michaelis, M. L. (2003) Oxidative Inactivation of Purified Plasma Membrane Ca^{2+}-ATPase by Hydrogen Peroxide and Protection by Calmodulin, *Biochemistry 42*, 12001−12010.
18. Zaidi, A., Gao, J., Squier, T. C., and Michaelis, M. L. (1998) Age-Related Decrease in Brain Synaptic Membrane Ca^{2+}-ATPase in F344/BNF1 Rats, *Neurobiol. Aging 19*, 487−495.
19. Xie, X. S., and Dunn, R. C. (1994) Probing Single Molecule Dynamics, *Science 265*, 361−364.
20. Ha, T., Laurence, T. A., Chemla, D. S., and Weiss, S. (1999) Polarization Spectroscopy of Single Fluorescent Molecules, *J. Phys. Chem. B 103*, 6839−6850.
21. Warshaw, D. M., Hayes, E., Gaffney, D., Lauzon, A. M., Wu, J., Kennedy, G., Trybus, K., Lowey, S., and Berger, C. (1998) Myosin Conformational States Determined by Single Fluorophore Polarization, *Proc. Natl. Acad. Sci. U.S.A. 95*, 8034−8039.
22. Adachi, K., Yasuda, R., Noji, H., Itoh, H., Harada, Y., Yoshida, M., and Kinosita, K., Jr. (2000) Stepping Rotation of F1-ATPase Visualized Through Angle-resolved Single-fluorophore Imaging, *Proc. Natl. Acad. Sci. U.S.A. 97*, 7243−7247.
23. Sosa, H., Peterman, E. J., Moerner, W. E., and Goldstein, L. S. (2001) ADP-Induced Rocking of the Kinesin Motor Domain Revealed by Single-molecule Fluorescence Polarization Microscopy, *Nat. Struct. Biol. 8*, 540−544.
24. Forkey, J. N., Quinlan, M. E., Shaw, M. A., Corrie, J. E., and Goldman, Y. E. (2003) Three-dimensional Structural Dynamics of Myosin V by Single-molecule Fluorescence Polarization, *Nature 422*, 399−404.
25. Osborn, K. D., Singh, M. K., Urbauer, R. J. B., and Johnson, C. K. (2003) Maximum Likelihood Approach to Single-Molecule Polarization Modulation Analysis, *ChemPhysChem 4*, 1005−1011.
26. Osborn, K. D., Zaidi, A., Mandal, A., Urbauer, R. J. B., and Johnson, C. K. (2004) Single-Molecule Dynamics of the Calcium-Dependent Activation of Plasma-Membrane Ca^{2+}-ATPase by Calmodulin, *Biophys. J. 87*, 1892−1899.
27. Osborn, K. D., Bartlett, R. K., Mandal, A., Zaidi, A., Urbauer, R. J. B., Urbauer, J. L., Galeva, N., Williams, T. D., and Johnson, C. K. (2004) Single-Molecule Dynamics Reveal an Altered Conformation for the Autoinhibitory Domain of Plasma-Membrane Ca^{2+}-ATPase Bound to Oxidatively Modified Calmodulin, *Biochemistry 43*, 12937−12944.
28. Yao, Y., Gao, J., and Squier, T. C. (1996) Dynamic Structure of the Calmodulin-Binding Domain of the Plasma Membrane Ca-ATPase in Native Erythrocyte Ghost Membranes, *Biochemistry 35*, 12015−12028.
29. Allen, M. W., Urbauer, R. J. B., Zaidi, A., Williams, T. D., Urbauer, J. L., and Johnson, C. K. (2004) Fluorescence Labeling, Purification and Immobilization of a Double Cysteine Mutant Calmodulin Fusion Protein for Single-Molecule Experiments, *Anal. Biochem. 325*, 273−284.
30. Fabiato, A. (1988) Computer Programs For Calculating Total From Specified Free Or Free From Specified Total Ionic Concentrations In Aqueous Solutions Containing Multiple Metals And Ligands, *Methods Enzymol. 157*, 378−417.
31. Lanzetta, P. A., Alverez, L. J., Reinsch, P. S., and Candia, O. (1979) An Improved Assay for Nanomole Amounts of Inorganic Phosphate, *Anal. Biochem. 100*, 95−97.
32. Falchetto, R., Vorherr, T., and Carafoli, E. (1992) The Calmodulin-Binding Site of the Plasma Membrane Ca^{2+} Pump Interacts with the Transduction Domain of the Enzyme, *Protein Sci. 1*, 1613−1621.

BI050488M